From: MECHANICS OF SHEET METAL FORMING (1978)
Edited by Donald P. Koistinen and Neng-Ming Wang
Book available from: Plenum Publishing Corporation
227 West 17th Street, New York, N.Y. 10011

SHEET NECKING-III. STRAIN-RATE EFFECTS*

J. W. HUTCHINSON

Harvard University, Cambridge, Massachusetts

K. W. NEALE

Université de Sherbrooke, Sherbrooke, Quebec, Canada

ABSTRACT

The effect of material strain-rate dependence on necking retardation is examined for biaxially-stretched sheets. Rate-dependent versions of both flow theory and deformation theory are employed in an analysis of the growth of long-wavelength nonuniformities. Material strain-rate sensitivity is seen to substantially increase the predicted limit strains beyond their corresponding values for time-independent material response. We also discuss the influence of strain-rate dependence on imperfection-sensitivity and forming limit curves.

INTRODUCTION

In this third and final Part of our investigation of sheet necking, we concentrate on the influence of material strain-rate dependence on necking retardation. A relatively small amount of strain-rate dependence is known to lead to substantially increased straining prior to necking [1–3]. This phenomenon was discussed in [1] for an axisymmetric bar under uniaxial tension. Ghosh [2, 3] has also studied the effects of strain-rate sensitivity on necking. In particular, he has collected experimental data for flat strips under uniaxial tension which shows that the maximum amount of overall axial strain attained is strongly dependent on the material strain-rate sensitivity characteristics. In addition, he has developed an approximate analysis for this strip problem which agrees very well with the trend of experiments.

As emphasized in [1], necking in strain-rate sensitive materials is inherently a nonlinear process. While classical linearized analyses, such as those discussed in Part I, can provide useful information regarding the early development of

* *The material in this three-part paper was presented orally in Session II under the title "Constitutive Relations for Sheet Metal" and Session IV under the title "Sheet Necking: Influence of Constitutive Theory and Strain-Rate Dependence".*

References p. 283.

nonuniformities, they do not give meaningful estimates for limit strains. Alternatively, an approximate nonlinear analysis based on the long-wavelength simplification discussed in [1] for axisymmetric bars under uniaxial tension does reproduce the essential details of the phenomenon, and will be applied herein.

As in Part II, we shall examine in detail here the basic differences between the results obtained using J_2 flow theory of plasticity and those determined with a rate-dependent J_2 deformation-type theory. Marciniak *et al* [4] have considered the effects of strain-rate sensitivity on localized necking in sheets; their analysis employs J_2 flow theory only and is restricted to the biaxial tension range. The present analysis is valid for a wider range of strain states. We shall examine imperfection-sensitivity and, in particular, how material strain-rate dependence alters forming limit curves.

LONG-WAVELENGTH(M-K) ANALYSIS

As mentioned previously, it is essential that nonlinearities be properly accounted for in an analysis of the necking process when the material response is time-dependent. Here, our analysis is based on long-wavelength (M-K) simplification. This approximation was applied in Part II to examine the influence of nonhomogeneities on sheet necking. An examination of some of its limitations was given in Part I.

Throughout this study we shall employ the same notation as that used in Part II. The derivation of the basic relations here closely parallels the detailed development given in the Section on Long-wavelength Analysis of II. To avoid unnecessary repetition, we shall simply discuss those steps of that analysis which must be modified to account for strain-rate dependent material behavior. The assumptions of material incompressibility and initial isotropy also apply here.

As in Part II, we consider a thin sheet which is initially uniform except for the presence of a nonhomogeneity concentrated in a narrow band across the sheet (Fig. 1), and examine the growth of this initial nonuniformity as the uniform section of the sheet is loaded.

To describe time-dependent material response, the following true stress-natural strain relation replaces (II: 11)*

$$\sigma_e = K\epsilon_e{}^N\dot{\epsilon}_e{}^m \qquad \text{(deformation theory)} \tag{1}$$

$$\sigma_e = K\bar{\epsilon}^N\dot{\bar{\epsilon}}^m \qquad \text{(flow theory)} \tag{2}$$

Here, σ_e and ϵ_e (or $\bar{\epsilon}$) are the effective stress and effective strain, equal to the true stress and true (logarithmic) strain, respectively, in uniaxial tension, and $\dot{\epsilon}_e$ (or $\dot{\bar{\epsilon}}$) is the effective strain-rate. N and m denote the strain hardening and strain-rate hardening exponents. As in II, we shall employ two distinct symbols and definitions for effective strain. In the deformation theory analysis ϵ_e is used and is defined in total form as $\epsilon_e = (2\epsilon_i\epsilon_i/3)^{1/2}$, where ϵ_i are the principal values of logarithmic strain. The effective strain-rate $\dot{\epsilon}_e$ is the time rate of change of ϵ_e.

* *This denotes equation (11) of Part II.*

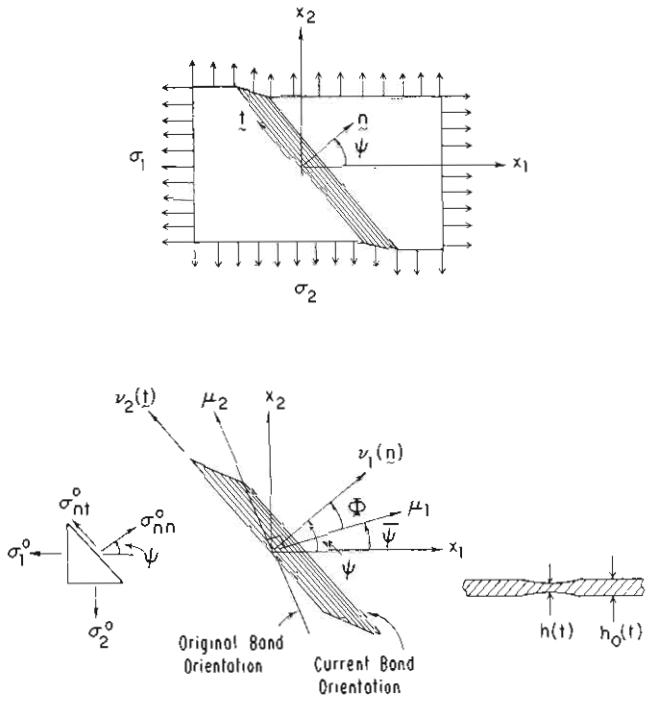

Fig. 1. Conventions.

Conversely, in the flow theory analysis we define the effective strain-rate in differential form as $\dot{\bar{\epsilon}} = (2\dot{\epsilon}_{ij}\dot{\epsilon}_{ij}/3)^{1/2}$, and the effective strain $\bar{\epsilon}$ is then the integral of $\dot{\bar{\epsilon}}$ with respect to time. In any monotonic proportional loading history $\epsilon_e = \bar{\epsilon}$.

Equation (1) or (2) brings in the effect of the strain-rate on the effective stress-strain relation in the simplest possible way. The constants K, N and m are those commonly determined from uniaxial test data. For multiaxial states for the rate-dependent "deformation theory", (1) is still supplemented by (II: 8), i.e.,

$$\epsilon_i = \mu s_i \tag{3}$$

where now μ depends on $\dot{\epsilon}_e$ through (1). The flow theory relation (II: 43), i.e.,

$$d\epsilon_{ij} = \frac{3}{2}\frac{d\bar{\epsilon}}{\sigma_e} s_{ij} \tag{4}$$

still goes with (2). For $m = 0$ both versions reduce to their counterpart relations used in Part II. Neither relation can be expected to adequately represent rate-dependent material behavior for arbitrary histories of stress or strain. But they can be expected to be reasonable generalizations of their respective time-independent limits for histories likely to be experienced in sheet-metal forming when stresses and strains increase monotonically with relatively slowly varying strain-rates. The rate-dependent flow theory, (2) and (4), is the same as that used by Marciniak *et al* [4]. We will refer to (1) and (3) as a rate-dependent "deformation

References p. 283.

theory'' in order to keep in mind its connection with the true deformation theory of Part II. In general, the rate-dependent version does not yield path-independent stress-strain behavior unless the effective strain-rate $\dot{\epsilon}_e$ is held constant.

The analysis producing equations (II: 33) to (II: 39) involves only equilibrium and the definition of strains so that these equations remain valid for the present investigation. However, in view of (1), (II: 40) is modified as follows, for deformation theory,

$$\frac{\sigma_{nn}^0/\sigma_e{}^0}{\sigma_{nn}/\sigma_e}\left(\frac{\dot{\epsilon}_e{}^0}{\dot{\epsilon}_e}\right)^m = (1-\xi)\left(\frac{\epsilon_e}{\epsilon_e{}^0}\right)^N \exp(\epsilon_3 - \epsilon_3{}^0) \tag{5}$$

with ϵ_e, $\epsilon_e{}^0$ and their rates replaced by $\bar{\epsilon}$, $\bar{\epsilon}^0$ and their rates for flow theory. Equation (II: 41) for the ratio $\sigma_{nn}^0/\sigma_e{}^0$ and (II: 42) for $\epsilon_3{}^0$ are unchanged.

J_2 Flow Theory Analysis—The flow theory relations (II: 43) to (II: 48) and (II: 50) to (II: 52) apply for the present analysis. However, since (5) replaces (II: 40), the expression analogous to (II: 49) becomes

$$(1-B-G)^{1/2}H\left[1-B\left(\frac{d\bar{\epsilon}^0}{d\bar{\epsilon}}\right)^2\right]^{-1/2}\left(\frac{d\bar{\epsilon}^0}{d\bar{\epsilon}}\right)^m = (1-\xi)\left(\frac{\bar{\epsilon}}{\bar{\epsilon}^0}\right)^N \exp(C\bar{\epsilon}^0 + \epsilon_3) \tag{6}$$

where (II: 51)

$$\frac{d\epsilon_3}{d\bar{\epsilon}^n} = -\frac{A}{H}\left[1-B\left(\frac{d\bar{\epsilon}^0}{d\bar{\epsilon}}\right)^2\right]^{1/2} - D\frac{d\bar{\epsilon}^0}{d\bar{\epsilon}} \tag{7}$$

The parameters A, B, C, D, G and H here depend only on the imposed strain ratio ρ and current band orientation ψ. For $\psi = 0$, the above equations reduce to those given by Marciniak *et al* [4].

From a straightforward incremental solution of (6) and (7), we can numerically determine the groove deformation $\bar{\epsilon}$ as a function of the prescribed uniform deformation $\bar{\epsilon}^0$. This numerical procedure is described more fully in II. Of particular interest here is the limit strain $\bar{\epsilon}^{0*}$, i.e., the maximum attainable strain in the uniform region of the sheet. As will be seen in the results which follow, the corresponding strain in the groove becomes unbounded, i.e., $\bar{\epsilon} \to \infty$, as $\bar{\epsilon}^0$ reaches its maximum value when the material response is strain-rate dependent.

J_2 Deformation Theory Analysis—The deformation-theory expressions (II: 53) to (II: 67) and (II: 69) are also valid for the present analysis. From (5), the modified form of (II: 68) becomes

$$\left[\frac{(\rho+2)\cos^2\psi + (2\rho+1)\sin^2\psi}{\sqrt{3}(1+\rho+\rho^2)^{1/2}}\right]\left(\frac{d\epsilon_e{}^0}{d\epsilon_e}\right)^m = \frac{(1-\xi)}{\lambda_1\lambda_2}\left(\frac{\epsilon_e}{\epsilon_e{}^0}\right)^N \exp(C\epsilon_e{}^0)\frac{Y}{\epsilon_e} \tag{8}$$

A step-wise numerical solution of this equation immediately gives the increments of ϵ_e in terms of the prescribed increments of $\epsilon_e{}^0$. At each step the current

values of principal stretches λ_i, groove angle ψ and principal axes orientation θ must be updated. The quantities λ_i and θ, however, depend on the parameters δ, γ, η and ϕ in (II: 53). From the matching conditions (II: 56), the current values of ϕ and γ are readily calculated. We compute δ and η in an incremental fashion by expressing (II: 65) and (II: 69) in rate form.

For the case $\bar{\psi} = \psi = 0$, the present analysis reduces to

$$(1 - B)^{1/2}\left[1 - B\left(\frac{\epsilon_e{}^o}{\epsilon_e}\right)^2\right]^{-1/2}\left(\frac{d\epsilon_e{}^o}{d\epsilon_e}\right)^m = (1 - \xi)\left(\frac{\epsilon_e}{\epsilon_e{}^o}\right)^N \exp(C\epsilon_e{}^o + \epsilon_3) \quad (9)$$

where ϵ_3 is given by (II: 72). The above relation (9) is analogous to (II: 71).

An interesting feature of the present analysis, both for flow theory and deformation theory, is that the relationship between $\epsilon_e{}^o$ and ϵ_e (or between $\bar{\epsilon}^o$ and $\bar{\epsilon}$) is independent of the load history experienced by the sheet and, in particular, is independent of the rate $\dot{\epsilon}_e{}^o(=\dot{\bar{\epsilon}}^o)$ at which the sheet is being deformed. Thus the limit strain for prescribed ρ and $\bar{\psi}$ is determined solely by the parameters m, N and ξ.

PLANE STRAIN CASE ($\rho = 0$)

For the plane strain case ($\rho = 0$), $\bar{\psi} = \psi = 0$ and, as in II, flow theory and deformation theory give identical predictions. In the long-wavelength analysis of the previous Section, $B = D = G = 0$, $H = 1$ and $A = C = \sqrt{3}/2$. Equations (7) or (II: 72) give $\epsilon_3 = -\sqrt{3}\epsilon_e/2 = -\epsilon_1$ and the relations (6) and (9) can be written as

$$(\epsilon_1{}^o)^{N/m} \exp(-\epsilon_1{}^o/m)d\epsilon_1{}^o = (1 - \xi)^{1/m}\epsilon_1{}^{N/m} \exp(-\epsilon_1/m)d\epsilon_1 \quad (10)$$

This relation is identical to the expression obtained in [1] for the axisymmetric bar under uniaxial tension, with ϵ_1 identified as the axial strain. The results and conclusions of that study are therefore directly applicable to the present problem. For $m = 0$, (10) reduces to (II: 74).

Typical results using (10) taken from [1] are shown in Fig. 2, where curves of $\epsilon_1/\epsilon_1{}^o$ are plotted against $\epsilon_1{}^o/N$ for an initial geometric nonuniformity $\xi = .005$. For the case $m = 0$, the curves are identical to those given in Fig. 4 of Part II. Of particular interest here is the limit strain, i.e., the maximum value of $\epsilon_1{}^o(=\epsilon_1{}^{o*})$ attained in the uniform region of the sheet. From (10) and this figure it can be seen that, when the material response is strain-rate dependent, the uniform strain $\epsilon_1{}^o$ reaches a maximum as the strain in the groove, ϵ_1, becomes unbounded. In contrast, for $m = 0$ the limiting value, which will be denoted by $\check{\epsilon}_1{}^{o*}$, is attained when $\epsilon_1 = N$ (see Part II).

The curves of Fig. 2 indicate that material strain-rate dependence greatly influences the maximum uniform strain that can be achieved. Fig. 3 illustrates this phenomenon for small values of strain-rate exponent ($m \leq .05$). Here,

$$\delta\epsilon_1{}^{o*} = \epsilon_1{}^{o*} - \check{\epsilon}_1{}^{o*} \quad (11)$$

is the increase, due to strain-rate dependence, of the limit strain in uniform region above the corresponding limit strain for a time-independent material ($m = 0$).

References p. 283.

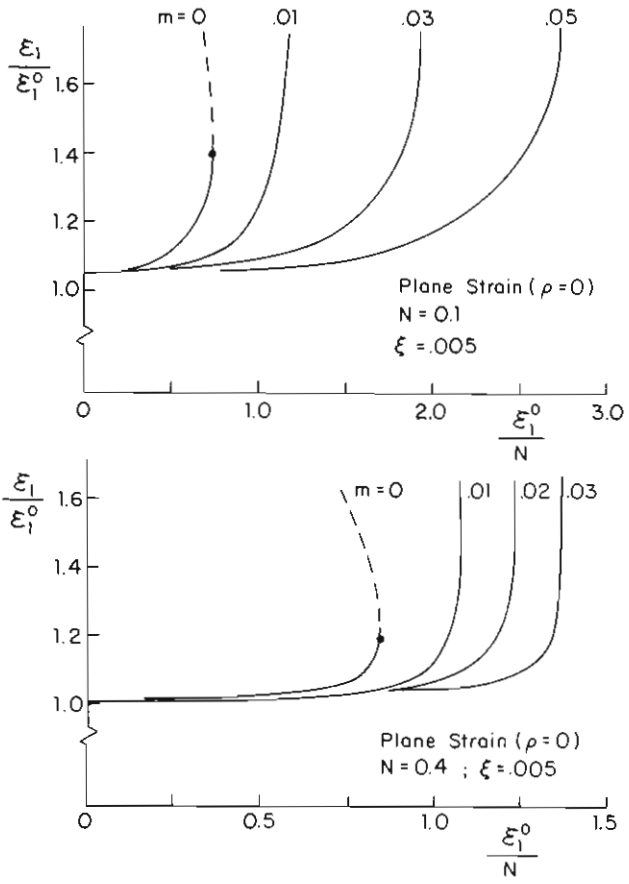

Fig. 2. Effect of strain-rate sensitivity index m on development of the strain in neck ϵ_1 as indicated by growth of ratio ϵ_1/ϵ_1^0, where ϵ_1^0 is the strain outside the neck.

As discussed in [1–3], very small values of m can lead to relatively large increases in ϵ_1^{0*}. It is also evident that $\delta\epsilon_1^{0*}$ decreases with increasing initial nonuniformity ξ, and increases with increasing strain-hardening exponent N. In fact, the numerical results depicted in Fig. 3 indicate that $\delta\epsilon_1^{0*}$ is nearly proportional to $\sqrt{N}$ for small m, as suggested by the asymptotic formula (12) given below.

In Fig. 4 the increase in limit strains for $m = .05$ are plotted against the initial imperfection ξ. (Curves of limit strain $\tilde{\epsilon}_1^{0*}(m = 0)$ vs. ξ for these cases can be found in Fig. 5 of Part II.) As mentioned above, the delay in necking $\delta\epsilon_1^{0*}$ decreases as the imperfection ξ increases. A basic difference between necking in time-dependent and time-independent materials can also be seen in Fig. 4. As $\xi \to 0$, the limit strain $\tilde{\epsilon}_1^{0*}$ approaches a finite value $(=N)$ when $m = 0$. In contrast, when the material response is time-dependent $(m \neq 0)$, $\epsilon_1^{0*} \to \infty$ as $\xi \to 0$. It is for this reason that $\delta\epsilon_1^{0*}$ becomes infinite at $\xi = 0$.

The numerical results of Figs. 2–4 indicate that very small values of strain-rate exponent m can substantially increase the limit strain ϵ_1^{0*} beyond its time-inde-

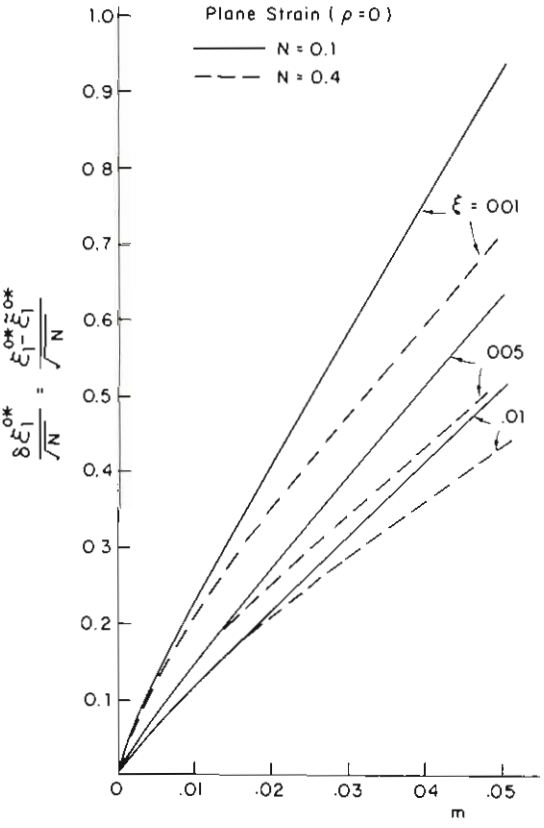

Fig. 3. Necking retardation due to small amounts of strain rate sensitivity as measured by the increase of the limit strain outside the neck over the time-independent value at $m = 0$.

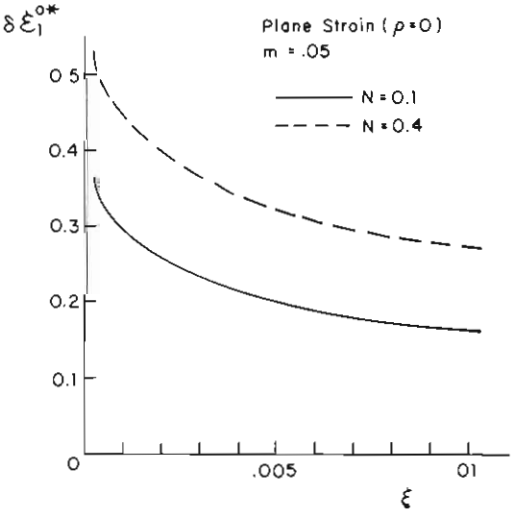

Fig. 4. Imperfection-sensitivity of additional limit strain in plane strain with $m = 0.5$. (Deformation theory and flow theory predictions coincide for $\rho = 0$.)

References p. 283.

pendent value $\bar{\epsilon}_1{}^{o*}$. An analysis was carried out in [1] to determine an exact asymptotic relation for the influence of very small m on $\epsilon_1{}^{o*}$. The result of that analysis, also valid for the present problem, is

$$\frac{\delta\epsilon_1{}^{o*}}{\sqrt{N}} \simeq \frac{m}{2\sqrt{2\xi}} \ln\left(\frac{4\pi\xi}{m}\right) \tag{12}$$

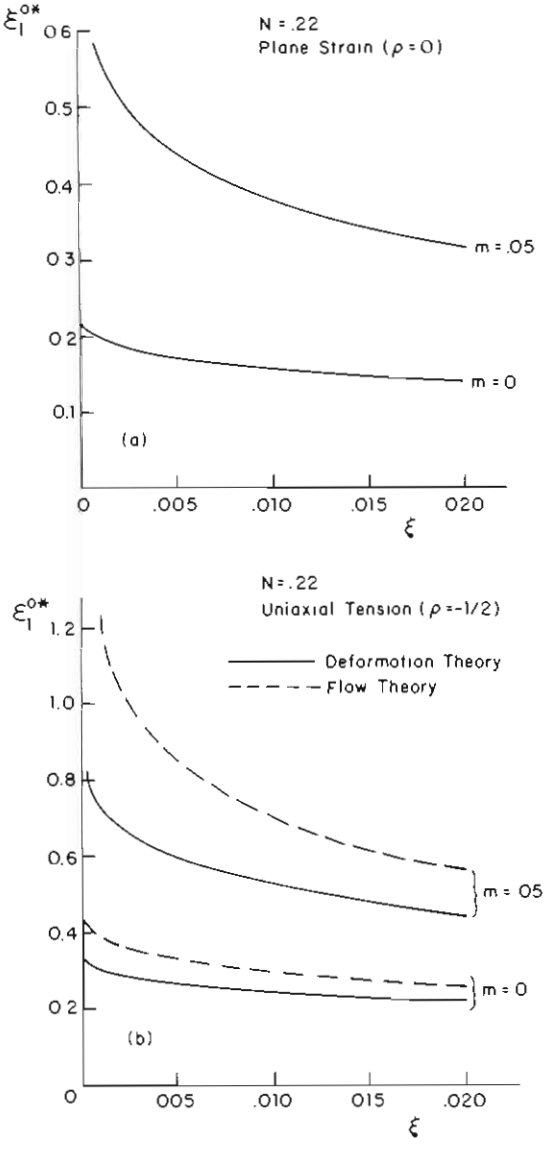

Fig. 5. Imperfection-sensitivity for two plasticity theories for time-independent limit (m = 0) and for m = .05: (a) plane strain, (b) uniaxial tension, (c) equibiaxial tension.

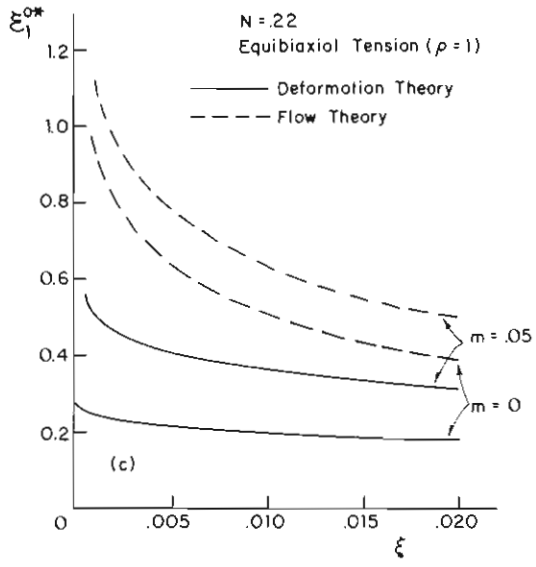

Here it is assumed that $\xi \ll 1$, $m < 2\xi$ and that m/N is small. This asymptotic relation has a rather restricted range of applicability. Nevertheless, it does reveal that the slope of the $\delta\epsilon_1{}^{o*} - m$ relation is infinite at $m = 0$, thereby illustrating a very strong dependence on m. It also indicates that $\delta\epsilon_1{}^{o*}$ is proportional to $\sqrt{N}$ for small m, as do the numerical results in Fig. 3. Furthermore, equation (12) implies that the amount of increase $\delta\epsilon_1{}^{o*}$ is quite sensitive to small variations in imperfection values ξ. We expect this since, as seen in Fig. 4, $\delta\epsilon_1{}^{o*}$ becomes infinite as $\xi \to 0$.

RESULTS AND DISCUSSION FOR FULL RANGE OF ρ

The long-wavelength relations (6), (7) for flow theory, and (8) for deformation theory, together with the condition ϵ_e (or $\bar{\epsilon}$) $\to \infty$ at $\epsilon_e{}^o = \epsilon_e{}^{o*}$, were used to investigate the influence of strain-rate sensitivity on limit strains. The range of strain ratios $-1/2 \leq \rho \leq 1$ was considered. Computations were carried out with various values of initial band orientation $\bar{\psi}$ to find the critical angle $\bar{\psi}^*$ giving the minimum limit strain. In the biaxial tension range ($\rho \geq 0$) this angle is $\bar{\psi}^* = 0$.

In Figs. 5(a)–(c) the variation of limit strain $\epsilon_1{}^{o*}$ with initial nonuniformity ξ is shown for $\rho = 0$, $-1/2$ and 1, respectively, and $N = .22$. Time-independent results ($m = 0$) taken from Part II are included here for comparison. A strain-rate hardening exponent $m \leq .05$ is typical of most common sheet metals at room temperature.

For the plane strain case ($\rho = 0$, Fig. 5(a)) there is no distinction between the predictions of flow theory and deformation theory, as mentioned in the previous Section. The curve for $m = 0$ exhibits the imperfection-sensitivity characteristics

References p. 283.

discussed in II. A much stronger imperfection-sensitivity is observed for the strain-rate dependent results ($m = .05$) since, as stated earlier, ϵ_1^{o*} becomes infinite as $\xi \to 0$. We also see that the limit strains for $m = .05$ are considerably higher than their corresponding values for $m = 0$.

The curves of ϵ_1^{o*} vs. ξ for uniaxial tension ($\rho = -1/2$, Fig. 5(b)) also exhibit

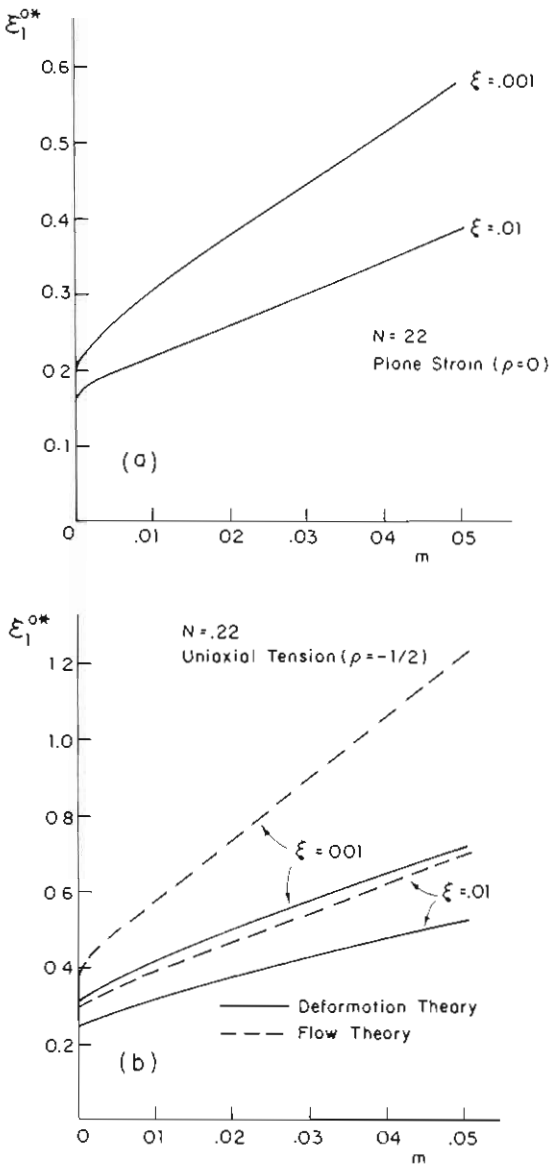

Fig. 6. Dependence of limit strain outside neck on strain-rate index for two plasticity theories: (a) plane strain, (b) uniaxial tension, (c) equibiaxial tension.

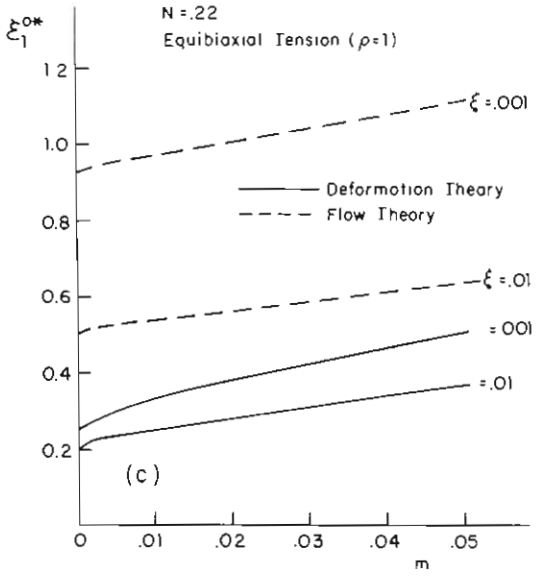

imperfection-sensitivity characteristics. Here, the solid and dashed curves refer to the deformation theory and flow theory predictions, respectively. For m = 0, the flow theory limit strains are somewhat higher and slightly more imperfection-sensitive than the corresponding deformation theory results as discussed in II. Both theories predict approximately the same *relative* increase in ϵ_1^{o*} due to strain-rate dependence (m = .05).

For the equibiaxial tension case (ρ = 1, Fig. 5(c)), a much larger discrepancy between the flow theory and deformation theory predictions is observed. As discussed in II, the flow theory limit strains for m = 0 are substantially higher than those based on deformation theory, and there is also considerably more imperfection-sensitivity associated with flow theory. With material strain-rate dependence (m = .05) the increase in limit strain for a given imperfection ξ is greater for deformation theory than for flow theory. Nevertheless, strain-rate effects do not raise the deformation theory predictions to the level of the time-independent flow theory results.

In Figs. 6(a)–(c) the dependence of limit strain ϵ_1^{o*} on strain-rate exponent m is illustrated for ξ = .01, .001 and ρ = 0, −1/2, and 1. Fig. 6(a) for plane strain shows the same trend as Fig. 3, namely, that strain-rate effects substantially increase limit strains beyond their time-independent values and that the amount of increase diminishes with increasing ξ. Figures 6(b) and 6(c) bring out the discrepancies between flow theory and deformation theory discussed previously. The uniaxial tension results of Fig. 6(b) indicate that the difference between both theories is greater for the lower values of ξ and higher values of m. The enormous discrepancy for the equibiaxial tension case is illustrated in Fig. 6(c).

Figs. 7(a) and 7(b) depict the manner in which the limit strain ϵ_1^{o*} under

References p. 283.

uniaxial tension varies with initial band orientation $\bar{\psi}$, as well as current groove orientation ψ^* at necking. Again, solid curves represent deformation theory predictions and dashed lines refer to flow theory. In these figures the values given in parentheses adjacent to each curve refer to m and ξ, respectively. The time-independent curves ($m = 0$) here are taken from II and, as mentioned there, they indicate that the flow theory limit strains are much more sensitive to variations in $\bar{\psi}$ and ψ^* than the predicted deformation theory results. With strain-rate dependence ($m = .05$) this sensitivity is accentuated for flow theory, particularly for smaller ξ, while the limit strains according to deformation theory are still rather unaffected by small changes in $\bar{\psi}$ or ψ^*.

In Fig. 7(a) it can be seen that the critical value of $\bar{\psi}$ which minimizes ϵ_1^{0*} with flow theory is greatly decreased by material strain-rate dependence, especially as the imperfection ξ is lowered. This effect, counteracted by the tendency of limit strain to increase as m is varied from $m = 0$ to .05, gives current minimizing values of ψ^* that do not vary substantially (see Fig. 7(b)). The corresponding variations in critical ψ^* for different m and ξ according to deformation theory are somewhat larger.

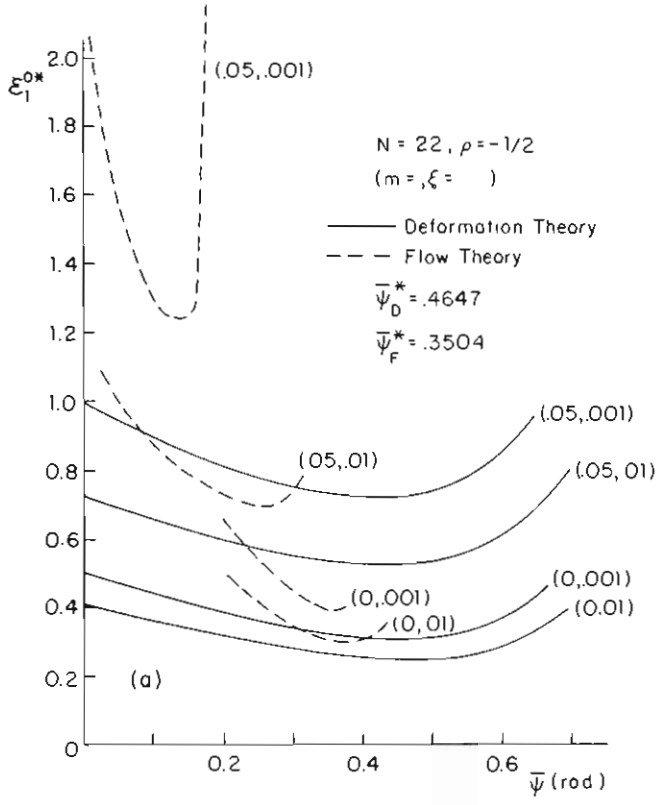

Fig. 7. Dependence on limit strain outside neck on orientation of necking band: (a) plotted against initial orientation angle $\bar{\psi}$, (b) plotted against final orientation angle ψ^*.

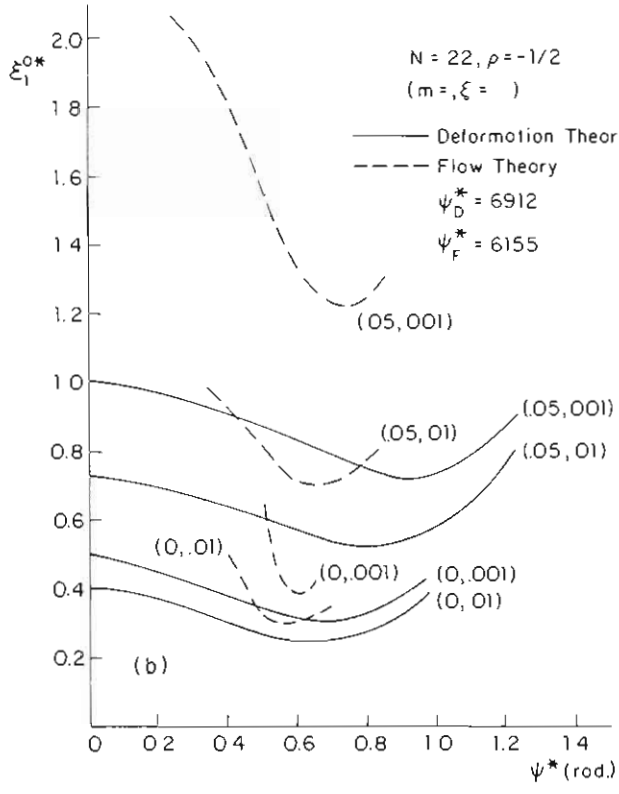

The effect of material strain-rate dependence on forming limit curves is depicted in Figs. 8 and 9 for strain-hardening exponents $N = .22$ and $.50$, respectively, and an imperfection level $\xi = .01$. Part II results for time-independent material response ($m = 0$) are also included here.

In the range $-1/2 \leq \rho \leq 0$, the shapes of the forming limit curves in Figs. 8 and 9 for $m = .05$ closely resemble the time-independent curves. The effect of increasing m in this range is essentially to just shift the forming limit curve upwards. In the biaxial tension range ($0 \leq \rho \leq 1$), however, there is a flattening of the curves due to strain-rate dependence. Nevertheless, the flow theory curves still rise rather steeply for $m = .05$ and both N-values, whereas the corresponding forming limit curves with deformation theory fall with increasing ρ.

A detailed discussion of the theoretical forming limit curves and their relationship to published experimental data was presented in Part II of this paper which dealt with time-independent material behavior. The outcome of the discussion on the issue of flow theory vs. deformation theory was the contention that deformation theory seems to give better qualitative agreement with experiments than does flow theory for the overall straining histories considered here. In particular for $\rho \geq 0$, where the discrepancies between theories are greatest, only deformation theory predicts the experimental trends of (i) a slightly rising forming limit

References p. 283.

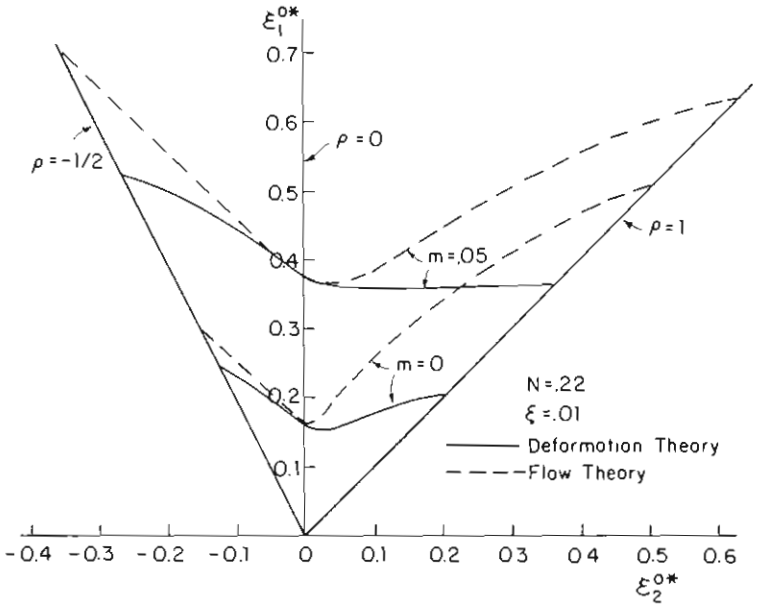

Fig. 8. Forming limit curves for $N = .22$ for two plasticity theories showing influence of strain-rate dependence.

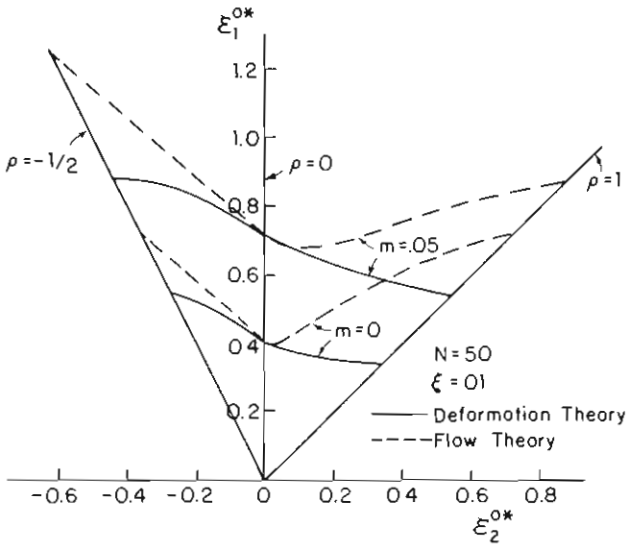

Fig. 9. Forming limit curves for $N = .50$ for two plasticity theories showing influence of strain-rate dependence.

curve for the lower N-values ($\leq .25$), or (ii) a curve which falls somewhat for the higher N-values ($\geq .50$). The results of the present study indicate that, even when strain-rate effects are incorporated in the analysis, simple flow theory does not predict this tendency.

ACKNOWLEDGMENT

The work of J.W.H. was supported in part by the Air Force Office of Scientific Research under Grant AFOSR 77-3330, the National Science Foundation under Grant ENG76-04019, and by the Division of Applied Sciences, Harvard University. The work was conducted while K.W.N. was on leave at Harvard University. The support of the Faculty of Applied Sciences at the University of Sherbrooke is gratefully acknowledged.

REFERENCES

[1] J. W. Hutchinson and K. W. Neale, Acta Met., *25* (1977), 839.
[2] A. K. Ghosh, J. Eng. Mater. Technol. (Trans. ASME, H), *99* (1977), 264.
[3] A. K. Ghosh, Research Publication GMR-2323, General Motors Research Laboratories, Warren, Mich. (1977).
[4] Z. Marciniak, K. Kuczyński and T. Pokora, Int. J. Mech. Sci., *15* (1973), 789.

DISCUSSION

A. K. Ghosh *(Rockwell International)*

Why did you choose Roger Pearce's data on brass for the negative side—why not our data? The way Roger Pearce conducted these tests, he takes a wide strip, cuts a slot in the strip for the negative side (slots of various width to height ratios) and the grid size is fixed. So as he moves closer to plane strain, because the grid size is fixed, you get strain gradients. And this is why I feel the negative side is not as steep as our results by punch stretching. He comes off to much higher plane-strain values.

Neale

In fact, I tried to qualify the discussion. There are a number of things which you do in an experiment which don't correspond to the very simple analysis that I've given here: we assume, for example, proportional straining in all regions of the sheet.

The other thing is that even though some experimental results, in the negative ρ range, might agree very well with Hill's calculations, I think it's hard sometimes to reconcile these results with the flow theory of plasticity because often when we do a test we are restricting the angle at which the neck eventually forms. Now as I showed on the slide (although I didn't discuss it in relation to experi-

ments) flow theory analysis results are highly sensitive to the angle at which necking does occur. So, if, in a test, we were constraining the angle quite a bit, to be zero for example, and if you work out the flow theory prediction it will give a prediction of limit strain much higher than Hill's results. However, deformation theory, as you saw, is fairly insensitive to this variation in angle.

S. P. Keeler *(National Steel Company)*

It bothers me that you use an fcc for a high N (in your notation) and a bcc for low N. What would happen if you had identical N values, let's say 0.2, and comparing a ferrons behavior versus a brass behavior? As Ghosh, Hecker, Azrin, and others have shown, you get two different behaviors with the same N value. How do you handle that problem?

Neale

In this analysis, we are using the simple, classical constitutive laws of plasticity. The only variable, at least in this analysis, is the strain hardening parameter N. We can use refined constitutive laws (continuum plasticity laws) as Prof. Hutchinson discussed yesterday, which take into account anisotropy, or we can develop models such as the ones that Prof. Rice discussed earlier, to model microscopic fracture. I think that's probably the only way. This analysis is based on a certain constitutive law, a certain continuum approach and if you want to model other types of material behavior, you will have to use a different constitutive law.

U. S. Lindholm *(Southwest Research Institute)*

We're new to the forming area but we've done a lot of multiaxial testing on tubular-type specimens and plotted many strain-to-failure diagrams which are essentially equivalent to the forming limit diagram if you assume the instability point and the failure strain are close approximations to one another. For ductile titanium, our data would seem to indicate in both quadrants (less than zero and greater than zero) that forming is more closely approximated by the flow theory. This is also true for beryllium but there the failure is more of a brittle failure than ductile failure, particularly if a more biaxial (1 to 1) strain ratio is imposed.

P. B. Mellor *(University of Bradford, U.K.)*

I think we are making great progress in learning how ignorant we are. I must, I'm afraid, complicate the situation even more. We've just completed some tests on brass using the Marciniak technique and we get a rising curve from plane strain to balanced biaxial tension which agrees fairly closely with the work which has been done in brass in that quadrant on curved specimens. So, I don't know how we determine that. We have been subjected to considerable discussion of strain rate during recent days, and I have just one query about the use of the expression for stress, strain and strain rate. Really it doesn't affect the result of

this theoretical paper but when we're actually getting the N value to feed into there, how can we get the N value? Because the N value you get from your stress strain curve itself for aluminum or steel does depend on the speed of testing, in fact on the strain rate. So I'm not quite sure. . . .

Neale

Well, I think it's the other term in the expression (the m value for strain rate sensitivity) which indicates the way your stress-strain curve does vary with speed of testing.

Mellor

Yes, but on the experimental side, I've not really seen any great data from which the N and m values have been calculated.

John Hutchinson *(Harvard University)*

I'm sure some of the experimentalists here could answer this much better than I. My understanding is that there is a fairly standard series of tests and it's a series of tests precisely. You take a tensile specimen say, and pull it at some fixed strain rate. Then you repeat the test at slightly higher strain rates and do a sequence of such tests. Then on two log-log plots, you pick the N and the M which best fit the slopes of the corresponding log-log plots. I believe that's what done.